Kinetic and Magnetic Resonance Studies of Effects of Genetic Substitution of a Ca^{2+}-Liganding Amino Acid in Staphylococcal Nuclease†

Engin H. Serpersu, David Shortle, and Albert S. Mildvan*
Department of Biological Chemistry, Johns Hopkins University School of Medicine, Baltimore, Maryland 21205
Received July 23, 1985

ABSTRACT: The X-ray structure of staphylococcal nuclease suggests octahedral coordination of the essential Ca^{2+}, with Asp-21, Asp-40, and Thr-41 of the enzyme providing three of the six ligands [Cotton, F. A., Hazen, E. E., Jr., & Legg, M. J. (1979) *Proc. Natl. Acad. Sci. U.S.A. 76*, 2551-2555]. The Asp-40 codon was mutated to Gly-40 on the gene that had been cloned into *Escherichia coli*, and the mutant (D40G) and wild-type enzymes were both purified from *E. coli* by a simple procedure. The D40G mutant forms a (5 ± 2)-fold weaker binary complex with Ca^{2+} as found by kinetic analysis and by Ca^{2+} binding studies in competition with Mn^{2+}, a linear competitive inhibitor. Similarly, as found by electron paramagnetic resonance (EPR), Mn^{2+} binds to the D40G mutant with a 3-fold greater K_D than that found with the wild-type enzyme. These differences in K_D are increased by saturation of staphylococcal nuclease with the DNA substrate such that K_m^{Ca} is 10-fold greater and K_I^{Mn} is 15-fold greater for the mutant than for the wild-type enzyme, although K_M^{DNA} is only 1.5-fold greater in the mutant. The six dissociation constants of the ternary enzyme-Mn^{2+}-nucleotide complexes of 3',5'-pdTp and 5'-TMP were determined by EPR and by paramagnetic effects on $1/T_1$ of water protons, and the dissociation constants of the corresponding Ca^{2+} complexes were determined by competition with Mn^{2+}. Only small differences between the mutant and wild-type enzymes are noted in K_3, the dissociation constant of the nucleotides from their respective ternary complexes. 3',5'-pdTp raises the affinities of both wild-type and mutant enzymes for Mn^{2+} by factors of 47 and 31, respectively, while 5'-TMP raises the affinities of the enzymes for Mn^{2+} by smaller factors of 6.8 and 4.4, respectively. Conversely, Mn^{2+} raises the affinities of both wild-type and mutant enzymes for the nucleotides by 1-2 orders of magnitude. Analogous effects are observed in the ternary Ca^{2+} complexes. Dissociation constants of Ca^{2+} and Mn^{2+} from binary and ternary complexes, measured by direct binding studies, show reasonable agreement with those obtained by kinetic analysis. Structural differences in the ternary metal complexes of the D40G mutant are revealed by a 31-fold decrease in V_{max} with Ca^{2+} and by 1.4-3.1-fold decreases in the enhancement of $1/T_1$ of water protons with Mn^{2+}. The frequency dependence of $1/T_1$ indicates a shorter correlation time in the mutant, resulting from a decrease in the symmetry and rigidity of the ligands of Mn^{2+}.

Staphylococcal nuclease [ribonucleate (deoxyribonucleate) 3'-nucleotidohydrolase, EC 3.1.4.7] is an extracellular 5'-phosphodiesterase of *Staphylococcus aureus* that can hydrolyze either DNA or RNA to yield 3'-mono- and dinucleotides (Tucker et al., 1978). Its relative simplicity, and its stability despite the absence of covalent cross-linkages, made the enzyme attractive for protein structure and enzyme function studies including X-ray crystallography. Staphylococcal nuclease is one of a small number of enzymes the structure of which has been determined at 1.5-Å resolution (Cotton et al., 1979). Although much structural information exists, the details of its catalytic mechanism remain unclear. The hydrolysis of DNA and RNA by staphylococcal nuclease appears to be completely dependent on the presence of Ca^{2+}. The hydrolysis of DNA, but not RNA, may occur with Sr^{2+} and to a much lesser degree with Fe^{2+} and Cu^{2+}. Though not activators, Mg^{2+} increases the velocity of the Ca^{2+} activated enzyme and Mn^{2+} has been shown to inhibit the Ca^{2+}-activated reaction, although the type of activation and inhibition, respectively, have not been elucidated (Cuatrecasas et al., 1967). The X-ray structure of a ternary enzyme-Ca^{2+}-3',5'pdTp complex reveals the metal to be in an octahedral environment, receiving three cis ligands from the protein, Asp-21, Asp-40, and Thr-41, as well as the 5'-phosphate of the competitive inhibitor, 3',5'pdTp. The remaining two ligands may be water molecules (Figure 1) (Cotton et al., 1979). No such structural information exists on the binary enzyme-Ca^{2+} complex.

The availability of site-specific mutants (Shortle, 1983; Shortle & Lin, 1985) and the extensive structural information available on staphylococcal nuclease led us to study the binding of Ca^{2+} and Mn^{2+} to the enzyme by employing EPR, NMR, and kinetic methods. The interactions of Ca^{2+}, Mn^{2+}, and nucleotides with both the wild-type and the mutant enzyme D40G, in which one of the metal binding residues, Asp-40, is replaced by glycine, are here investigated. Our results show significant differences in the metal binding properties of wild-type enzyme and D40G and, in addition, marked reduction in the maximal velocity of the mutant enzyme. For these studies, a simple purification procedure for staphylococcal nuclease from overproducing strains of *Escherichia coli* is here reported. A preliminary report of this work has been published (Serpersu et al., 1985).

Experimental Procedures

Materials

The nucleotides 5'-TMP and 3'-TMP were purchased from Sigma and 3',5'-pdTp was obtained from P-L Biochemicals. Before use, buffer and nucleotide solutions were passed over Chelex 100 resin to remove trace metals. Highly polymerized salmon sperm DNA and calf thymus DNA were purchased from Sigma, and all DNA used in the enzyme assays was

† This work was supported by National Institutes of Health Grants AM28616 and GM34171 and National Science Foundation Grant PCM8219464.

0006-2960/86/0425-0068$01.50/0

Table I: Purification of Wild-Type and Mutant (D40G) Staphylococcal Nuclease

enzyme	step	vol (mL)	[protein] (mg/mL)	total protein (mg)	sp act. (units/mg)[a]	total units	yield (%)	purification (x-fold)
wild type	extract	38	0.84	31.9	466	14852	100	1
	Bio-Rex 70	7.3	1.26	9.21	644	6155	41.4	1.43
	dialysis	10.0	0.63	6.30	678	4271	28.8	1.46
	lyophilized			5.90	672[b]	3965	26.7	1.44
D40G	extract	50	0.87	43.5	12.4	539	100	1
	Bio-Rex 70	7.5	1.25	9.4	23.5	220.9	40.9	1.89
	dialysis	10.0	0.64	6.4	22.7	145.3	26.9	1.83
	lyophilized			5.9	23.0[c]	135.7	25.2	1.85

[a] Determined in 40 mM Tris-HCl, pH 7.4. [b] Was 2700 units/mg in 40 mM sodium borate buffer, pH 8.8. [c] Was 37 units/mg in 40 mM sodium borate buffer, pH 8.8.

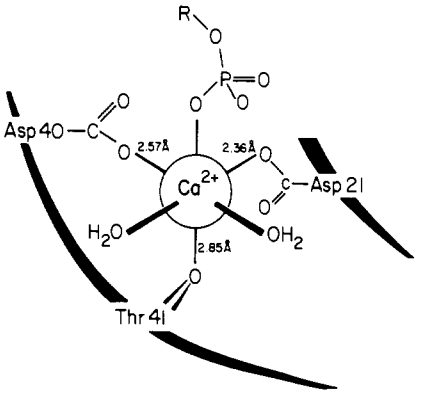

FIGURE 1: Ligands of Ca^{2+} at the active site of staphylococcal nuclease, on the basis of the 1.5-Å structure of the ternary enzyme–Ca^{2+}–pdTp complex (Cotton et al., 1979). In the absence of pdTp, a third water ligand probably occupies the position of the phosphate ester.

denatured by heating for 30 min at 100 °C, followed by rapid cooling on ice (Cuatrecasas et al., 1967).

Methods

Enzyme Assay. The enzyme activity was measured by observing the absorbance change at 260 nm (Cuatrecasas et al., 1967). One unit of enzymatic activity is defined as the amount of the enzyme causing a change of 1.0 absorbance unit per minute at 260 nm in a 1-cm cell. Protein concentrations were determined by absorbance at 280 nm ($\epsilon_{1cm}^{0.1\%} = 0.93$ at neutral pH) (Dunn et al., 1973; Tucker et al., 1978). The assay mixture consisted of the indicated amounts of DNA and Ca^{2+} in 40 mM Tris-HCl,[1] pH 7.4, in a volume of 1.0 mL at 23.5 °C. To this mixture, either 0.08–0.1 μg of wild-type enzyme or 1.8–2.3 μg of D40G was added to start the reaction. Velocity was determined from the linear portions of the recorder trace and expressed as absorbancy per minute per microgram of protein. Enzyme activities were linear with the amount of protein used in the assays. In the kinetic experiments with Mn^{2+} as inhibitor, the concentration of free Mn^{2+} was estimated by assuming 0.38 ± 0.04 Mn^{2+} binding sites per DNA phosphorus with a dissociation constant of 68 μM (Slater et al., 1972).

Isolation of Wild-Type and Mutant D40G Staphylococcal Nuclease. The structural genes of the wild-type and mutant (D40G) forms of staphylococcal nuclease were isolated and expressed in *E. coli* as previously described (Shortle & Lin, 1985). The engineered strain of *E. coli* carrying the plasmid pFOG405 for both the wild-type form and the D40G mutation was grown overnight in LB medium (10 g of Bacto tryptone + 5 g of Bacto yeast extract + 10 g of NaCl in 1 L) containing 50 μg/mL ampicillin at 37 °C. The cultures were then diluted 50-fold into complete MOPS media, which consists of 200 mL of solution M (42 g of MOPS + 4 g of Tricine + 14.6 g of NaCl + 8 g of KOH + 2.55 g of NH_4Cl in 1 L), 2 mL of solution O (26.8 g of $MgCl_2 \cdot 6H_2O$ + 10 mL of a solution containing 8 mL of concentrated HCl, 5 g of $FeCl_2 \cdot 4H_2O$, 184 mg of $CaCl_2 \cdot 2H_2O$, 64 mg of H_3BO_3, 40 mg of $MnCl_2 \cdot 4H_2O$, 18 mg of $CoCl_2 \cdot 6H_2O$, 4 mg of $CuCl_2 \cdot 2H_2O$, 340 mg of $ZnCl_2$, and 605 mg of $Na_2MoO_4 \cdot 2H_2O$ taken to 1 L), 0.1 mL of 1.0 M KH_2PO_4, 1.0 mL of 0.276 M K_2SO_4, 20 mL of 20% glucose, 2 mL of 0.05% thiamine, 20 mL of 7.5% vitamin-free casein hydrolysate, and H_2O to 1 L. The cells containing the wild-type form were further incubated for 5 h and those containing D40G for 7 h at 37 °C with shaking.

At the end of the incubations, the cells were pelleted by centrifugation at 9000*g* for 10 min and resuspended in 1/40 the original volume of ice-cold 1 M Tris base (pH ~10.5) containing 2.5 mM Na^+EDTA. They were incubated on ice for 20 min with intermittent gentle swirling. Again the cells were pelleted, and the supernatant was removed carefully, without disturbing the cells. To the supernatant, 1/10 volume of 1 M HEPES (acid form) was added. This lowers the pH of the extract to approximately 9.2. The extract was then loaded onto a 1 × 20 cm Bio-Rex 70 column, which had been equilibrated with a buffer made of 10 parts of 1 M Tris base, containing 2.5 mM Na^+EDTA, and 1 part of 1 M HEPES (acid form), the final pH of which was 9.2. Under these conditions, the Bio-Rex 70 (100–200 mesh) had a capacity of 2–5 mg of nuclease/mL of bed volume. The column was washed with 1–2 bed volumes of the same buffer, followed by 5 bed volumes of 0.2 M Tris-HCl, pH 7.6. The enzyme was eluted in 1.5 bed volumes of 1 M Tris-HCl, pH 7.6, containing 0.5 M NaCl. After exhaustive dialysis against 100 volumes of 2 mM Tris-HCl, pH 7.4, with four changes, the enzymes were lyophilized and stored at −70 °C.

Both the wild-type and D40G enzymes were homogeneous as judged by their migration as single bands on SDS–PAGE. The final specific activity of the wild-type enzyme was 644 ± 9 units/mg at pH 7.4, in agreement with that found for a pure preparation from Worthington Biochemicals (641 ± 15 units/mg), while the specific activity of pure D40G was 16.7 ± 1.6 units/mg under these conditions. When assayed in 40 mM sodium borate buffer, pH 8.8, the specific activity of the wild-type enzyme was 2700 units/mg, which is somewhat greater than the value of 2000 units/mg previously reported for the pure enzyme (Cuatrecasas et al., 1967). The specific activity of the D40G mutant under these conditions was 37 units/mg. Table I summarizes the purification of the wild-type and mutant enzymes, respectively.

Magnetic Resonance Measurements. The longitudinal relaxation rate of water protons was measured with a Nuclear

[1] Abbreviations: 3′,5′-ϵpAp, 1,N^6-ethenoadenosine 3′,5′-bisphosphate; Tris-HCl, tris(hydroxymethyl)aminomethane hydrochloride; MOPS, 3-(*N*-morpholino)propanesulfonic acid; Tricine, *N*-[tris(hydroxymethyl)methyl]glycine; EDTA, ethylenediaminetetraacetic acid; HEPES, 4-(2-hydroxyethyl)-1-piperazineethanesulfonic acid; SDS–PAGE, sodium dodecyl sulfate–polyacrylamide gel electrophoresis.

Table II: Kinetic Parameters of Wild-Type and Mutant (D40G) Staphylococcal Nuclease[a]

	K_M^{Ca} (μM)	K_M^{DNA} (μg/mL)	K_A^{Ca} (μM)	K_S^{DNA} (μg/mL)	K_I^{Mn} (μM)	V_{max} (ΔAbs min^{-1} μg^{-1})
wild type	110 ± 20	3.5 ± 0.8	460 ± 60	17.9 ± 0.7	6.8 ± 4.2	0.714 ± 0.040
mutant	1130 ± 70	4.65 ± 1.25	3440 ± 360	27.8 ± 3.4	105 ± 15	0.024 ± 0.002

[a] From Figures 2–4. K_M^{Ca} is the Michaelis constant of Ca^{2+} at saturating [DNA], K_M^{DNA} is the Michaelis constant of DNA at saturating [Ca^{2+}], K_A^{Ca} is the K_M of Ca^{2+} extrapolated to zero [DNA], and K_S^{DNA} is the K_M of DNA extrapolated to zero [Ca^{2+}].

Magnetic Resonance Specialties PS-60W pulsed NMR spectrometer at 24.3 MHz as described previously (Mildvan & Engle, 1972) by using the 180°–τ–90° pulse sequence method of Carr & Purcell (1954; Mildvan & Engle, 1972). The observed enhancement of relaxation rate is defined as $\epsilon^* = (1/T_{1p}^*)/(1/T_{1p})$, where $1/T_{1p}$ is the paramagnetic contribution to the relaxation rate in the presence (*) and absence of the enzyme (Mildvan & Engle, 1972).

The concentration of free Mn^{2+} in a mixture of free and bound Mn^{2+} was determined by electron paramagnetic resonance (Cohn & Townsend, 1954) with a Varian E-4 EPR spectrometer. The EPR and NMR data were analyzed as previously described (Mildvan & Cohn, 1963, 1966; Mildvan & Engle, 1972) to determine the stoichiometry (n) of Mn^{2+} ions bound to each enzyme, the dissociation constant (K_D), and the enhancement (ϵ_b) of the binary enzyme–Mn^{2+} complex. Titrations of the binary enzyme–Mn^{2+} complex with nucleotides were analyzed by computer as previously described (Reed et al., 1970; Mildvan & Engle, 1972) to yield dissociation constants and enhancement values of ternary complexes. In addition, the binding of Mn^{2+} to enzyme–nucleotide complexes was monitored by EPR and by changes in $1/T_{1p}^*$ of water protons, providing independent measurements of the dissociation constants of Mn^{2+} from ternary enzyme–Mn^{2+}–nucleotide complexes. The correlation time (τ_c) for dipolar interaction of enzyme-bound Mn^{2+} with water protons was determined from the frequency dependence of $1/T_{1p}$ (Reuben & Cohn, 1970).

Fluorescence Measurements. The dissociation constants of the binary complexes of staphylococcal nuclease with 3′,5′-pdTp were determined by competition with 3′,5′-ϵpAp, on the basis of the quenching of the ϵpAp fluorescence by the enzyme. Solutions containing 61 μM wild-type enzyme with 118 μM ϵpAp or 138 μM D40G enzyme with 104 μM ϵpAp in 40 mM Tris-HCl, pH 7.4, were titrated with 3′,5′-pdTp. The increase in fluorescence at 408 nm upon excitation at 307 nm was measured in an Aminco Bowman spectrofluorometer thermostated at 23 °C. Double-reciprocal plots of the changes in fluorescence intensity vs. pdTp concentration were fit by linear least-squares analysis.

Results

Kinetics of Activation by Ca^{2+}. Staphylococcal nuclease has a broad pH optimum in the range of 8.6–10.3, which depends on the concentration of Ca^{2+} (Tucker et al., 1978). Since the mutant enzyme D40G has enzymatic activity, we have determined the kinetic parameters of both enzymes at pH 7.4 at which Mn^{2+} binding studies can be performed, since Mn^{2+} precipitates at higher pH values. Figures 2 and 3 show detailed kinetic analyses of the activation by Ca^{2+} at varying levels of DNA of both the wild-type and mutant enzymes at pH 7.4. A comparison of the kinetic parameters (Table II) indicates that at saturating levels of DNA the mutant enzyme shows a 10-fold higher K_M value and a 31-fold lower maximum velocity than the wild-type enzyme. Extrapolation to zero DNA concentration yields activator constants for Ca^{2+} indicating a 7.5-fold weaker binding of Ca^{2+} to the mutant enzyme than to the wild-type enzyme in the binary enzyme–Ca^{2+}

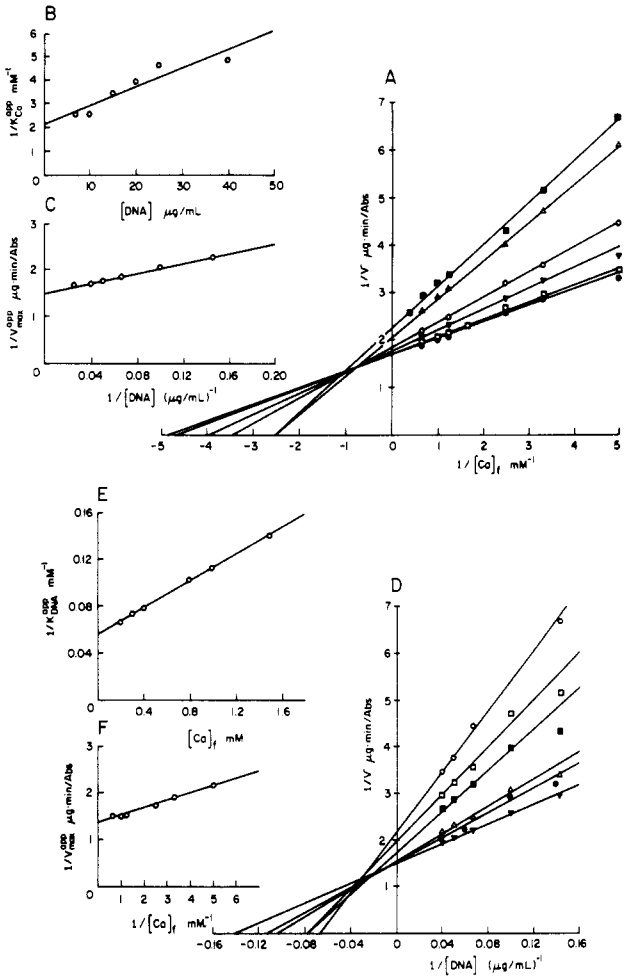

FIGURE 2: Kinetics of activation of wild-type staphylococcal nuclease by Ca^{2+}. (A) Double-reciprocal plot of initial velocity vs. Ca^{2+} concentration. DNA (salmon sperm) concentrations were (from top to bottom) 7 (■), 10 (▲), 15 (○), 20 (▼), 25 (□), and 40 μg/mL (●). The assay medium also contained 40 mM Tris-HCl, pH 7.4. The reaction in a total volume of 1.0 mL at 23.5 °C was started by the addition of 0.08 μg of the enzyme. The velocity of the reaction was defined as the absorbance change at 260 nm per microgram of enzyme per minute. (B) Secondary plot of reciprocal of extrapolated apparent K_M^{Ca} (K_{Ca}^{app}) values, obtained from the intercepts on the abscissa in (A), against DNA concentration. Extrapolation to zero DNA concentration yielded the activator constant of Ca^{2+} (K_A^{Ca}) as 0.46 mM. (C) Secondary plot of extrapolated apparent V_{max} at infinite Ca^{2+} concentration (V_{max}^{app}), against the DNA concentrations in double-reciprocal form. From the intercept on the abscissa, K_M^{DNA} = 3.5 μg/mL was obtained. (D) Double-reciprocal plot of initial velocity against DNA concentration. Ca^{2+} concentrations were (from top to bottom) 0.2 (○), 0.3 (□), 0.4 (■), 0.8 (▲), 1.0 (●), and 1.5 mM (▼). (E) Secondary plot of reciprocal of extrapolated apparent K_M^{DNA} (K_{DNA}^{app}) values, obtained from the intercepts on the abscissa in (D), against Ca^{2+} concentration. Extrapolation to zero Ca^{2+} concentration yielded the dissociation constant of DNA (K_S^{DNA}) as 17.9 μg/mL (or 12.8 μM, see Table V). (F) Secondary plot of extrapolated apparent V_{max} at infinite DNA concentration (V_{max}^{app}), against the Ca^{2+} concentration in double-reciprocal form. Intercept on the abscissa yielded K_M^{Ca} = 0.11 mM. In (A) and (D), the data points are shown together with the lines computed by a weighted least-squares analysis (Cleland, 1979). In (B), (C), (E), and (F), the lines are computed by a linear least-squares analysis.

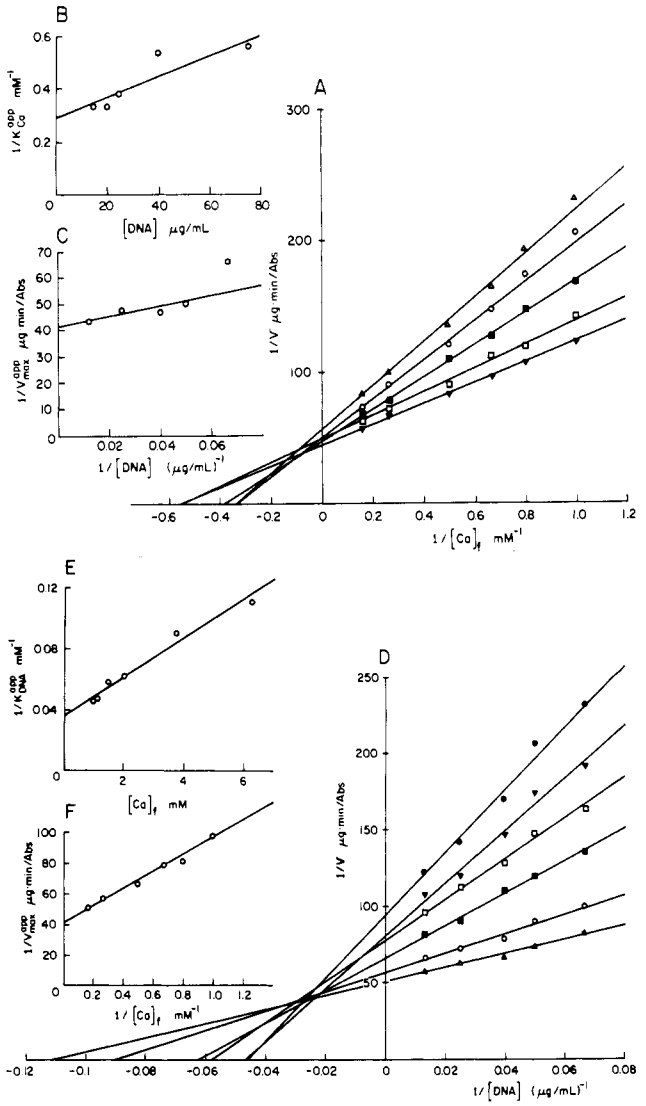

FIGURE 3: Kinetics of activation of the D40G mutant of staphylococcal nuclease by Ca^{2+}. (A) Double-reciprocal plot of initial velocity against Ca^{2+} concentration. DNA (salmon sperm) concentrations were 15 (△), 20 (○), 25 (■), 40 (□), and 75 μg/mL (▼). The assay conditions were otherwise as described in Figure 2 except that 1.8 μg of the D40G mutant enzyme per assay was used. (B) Secondary plot of the reciprocal of the extrapolated apparent K_M of Ca^{2+} (K_{Ca}^{app}) values, obtained from the intercepts on the abscissa in (A), against the DNA concentration. Extrapolation to zero DNA concentration yielded the activator constant of Ca^{2+} (K_A^{Ca}) as 3.44 mM. (C) Secondary plot of the extrapolated apparent V_{max} at infinite Ca^{2+} concentration (V_{max}^{app}), against the DNA concentration in double-reciprocal form. The intercept on the abscissa yielded K_M^{DNA} = 4.65 μg/mL. (D) Double-reciprocal plot of the initial velocity against DNA concentration. Ca^{2+} concentrations were (from top to bottom) 1.0 (●), 1.25 (▼), 1.5 (□), 2.0 (■), 3.75 (○), and 6.25 mM (△). (E) Secondary plot of the reciprocal of the extrapolated apparent K_M^{DNA} (K_{DNA}^{app}) values, obtained from the intercepts on the abscissa in (D), against the Ca^{2+} concentration. Extrapolation to zero Ca^{2+} concentration yielded the dissociation constant of DNA (K_S^{DNA}) as 27.8 μg/mL (or 19.9 μM, see Table V). (F) Secondary plot of the extrapolated apparent V_{max} at infinite DNA concentration (V_{max}^{app}), against the Ca^{2+} concentration in double-reciprocal form. The intercept on the abscissa yielded K_M^{Ca} = 1.33 mM. In (A) and (D), the data points are shown together with the lines computed by a weighted least-squares analysis. In (B), (C), (E), and (F), linear least-squares analyses were used.

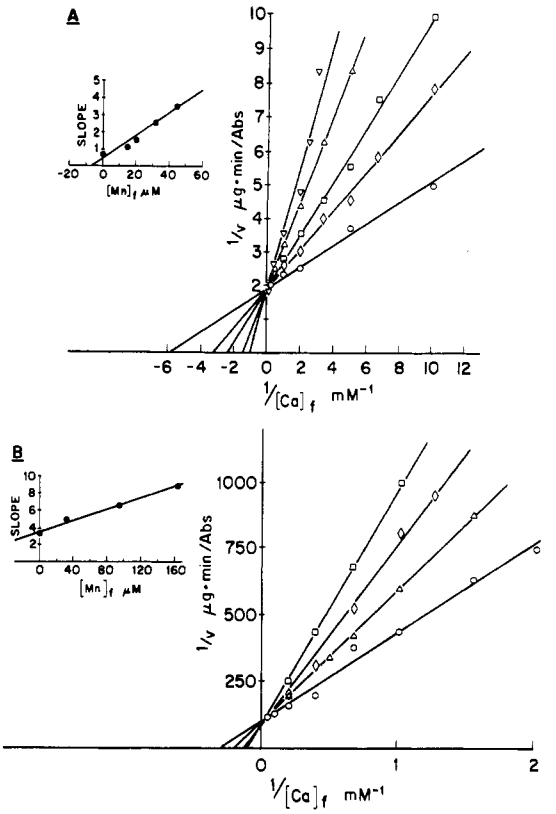

FIGURE 4: Kinetics of inhibition by Mn^{2+} of the wild-type enzyme and the D40G mutant of staphylococcal nuclease. (A) Double-reciprocal plot of initial velocity against Ca^{2+} and Mn^{2+} concentrations with the wild-type enzyme. Free Mn^{2+} concentrations were 0.0 (○), 14.8 (◇), 20.2 (□), 31.5 (△), and 44.5 μM (▽). The assay medium contained 40 mM Tris-HCl, pH 7.4, and 50 μg/mL of calf thymus DNA. The reaction in a total volume of 1.0 mL was started by the addition of 0.1 μg of the wild-type enzyme. Inset shows the secondary plot of slopes against free Mn^{2+} concentration, which yielded K_I^{Mn} = 6.8 μM. (B) Double-reciprocal plot of initial velocity against Ca^{2+} and Mn^{2+} concentrations with the D40G mutant. Free Mn^{2+} concentrations were 0.0 (○), 31.5 (△), 95 (◇), and 164 μM (□). The assay conditions were otherwise as in (A) except that the reaction was started by the addition of 2.1 μg of the D40G mutant enzyme. Inset shows the secondary plot of slopes against free Mn^{2+} concentrations, which yielded K_I^{Mn} = 105 μM. In (A) and (B), free Mn^{2+} was estimated as described under Experimental Procedures, and the data points are shown together with the lines computed by a weighted least-squares analysis. In both insets, linear least--squares analyses were used.

complex. Extrapolation to infinite DNA yields a 10-fold greater K_M of Ca^{2+} in the mutant enzyme, indicating weaker Ca^{2+} binding in the ternary complex as well. The large effect on V_{max} of the mutant was unaffected by the addition of 100 mM sodium formate in an attempt to replace the missing carboxylate group. The K_M values of the DNA substrates from Figures 2 and 3, and as measured independently, indicated only (1.4 ± 0.1)-fold weaker substrate binding to the mutant than to the wild-type enzyme.

Kinetic Effects of Mn^{2+}. No activation by Mn^{2+} was detected over the range 3.0–50 μM $MnCl_2$ at pH 7.4 with either the wild-type (5 μg/mL) or mutant enzymes (173 μg/mL). From the error levels of these measurements, activation by Mn^{2+} is less than 0.017% of that produced by Ca^{2+}, in accord with previous studies at high pH (Cuatrecasas et al., 1967). Mn^{2+} is, however, a linear competitive inhibitor with respect to Ca^{2+} of both the wild-type and mutant enzymes (Figure 4) with K_I values of 6.8 and 105 μM, respectively (Table II). Thus, the DNA complex of the wild-type enzyme binds Mn^{2+} 15-fold more tightly than does that of the mutant.

Mn^{2+} Binding Studies. To study the binary enzyme–Mn^{2+} complexes, both the wild-type enzyme and the D40G mutant of staphylococcal nuclease were titrated with Mn^{2+}. At each point of the titration, the free Mn^{2+} concentration was measured by EPR spectroscopy, and the enhancement (ϵ^*) of $1/T_{1p}$

Table III: Dissociation Constants of Binary Complexes of Mn^{2+} and Ca^{2+} and Enhancement Factors of Mn^{2+} Complexes

ligand	n^e	K_D^{Mn} or K_I^{Mn} (μM)^e	ϵ_b	K_D^{Ca} or K_I^{Ca} (μM)^e
wild type	0.95 ± 0.03[a]	416 ± 22[a]		510 ± 70[c]
	1.00 ± 0.05[b]	460 ± 63[b]	8.4 ± 0.7	
mutant	0.98 ± 0.07[a]	1250 ± 170[a]		1660 ± 300[c]
(D40G)	0.83 ± 0.03[b]	1012 ± 15[b]	3.8 ± 0.5	
5′-TMP	1.06 ± 0.05[a]	4130 ± 200[a]	1.54 ± 0.09	5100 ± 2500[d]
3′,5′-pdTp	1.6 ± 0.2[a]	474 ± 50[a]	1.7 ± 0.1	1200 ± 700[d]

[a] Determined by EPR, as in Figure 5A. [b] Determined by $1/T_{1p}^*$ of water protons. [c] Determined by competition with Mn^{2+} measuring $1/T_{1p}^*$ of water protons (Figure 6A). [d] Determined by competition with Mn^{2+} measuring free [Mn^{2+}] by EPR. [e] n is the stoichiometry of metal binding, K_D is the dissociation constant of the binary enzyme–metal complex, and K_I is the dissociation constant of the binary metal–nucleotide complex.

of water protons was determined by pulsed NMR. With the values for the fraction of free and bound Mn^{2+} determined by EPR spectroscopy, the data were analyzed by a Scatchard plot (Figure 5A), which could be fit by assuming one Mn^{2+} binding site for both the wild-type enzyme and the D40G mutant (Table III) with dissociation constants of 0.416 ± 0.022 and 1.25 ± 0.17 mM, respectively (Table III).

The enhancement of $1/T_{1p}$ of water protons (ϵ_b) resulting from Mn^{2+} binding to staphylococcal nuclease in the absence of nucleotides or substrates was found to be 8.4 ± 0.7 for the wild-type enzyme and significantly lower (3.8 ± 0.5) for D40G (Table III), indicating a structural difference in the coordination sphere of Mn^{2+}. The relaxation data were used independently to determine the stoichiometries and dissociation constants of Mn^{2+} from the wild-type and mutant enzymes. Within experimental error (Table III), the results agreed with those determined by EPR. The dissociation constants of the binary enzyme–Mn^{2+} complexes are significantly greater than the respective K_I values of Mn^{2+} (Table IV), indicating that the presence of DNA in the kinetic experiments raises the affinity of the wild-type and mutant enzymes for Mn^{2+} by factors of 61 and 12, respectively. Such tightening will be confirmed by studies of the binding of Mn^{2+} to enzyme–nucleotide complexes in a later section.

Displacement of Mn^{2+} from the Binary Enzyme–Mn^{2+} Complex by Ca^{2+}. The addition of Ca^{2+} to the binary Mn^{2+} complex of the wild-type and mutant enzymes decreased the observed enhancement, suggesting that Ca^{2+} displaces Mn^{2+} from both enzymes (Figure 6A). This point was established by EPR measurements, which detected the appearance of free Mn^{2+}. At high levels of Ca^{2+}, essentially all of the Mn^{2+} was displaced. From the amount of Ca^{2+} required to displace half of the bound Mn^{2+} and the measured dissociation constants of the enzyme–Mn^{2+} complexes (Table III), binary Ca^{2+}–enzyme dissociation constants of 0.51 ± 0.07 and 1.7 ± 0.3 mM for the wild-type enzyme and D40G, respectively, were estimated (Table III). These values are in reasonable agreement with the activator constants of 0.46 ± 0.06 and 3.4 ± 0.4 mM, respectively, obtained by the kinetic experiments (Table II).

Ternary Mn^{2+} Complexes of Wild-Type and D40G Enzymes with Nucleotide Substrate Analogues. (A) Titrations with Mn^{2+}. The thermodynamics of a ternary system of enzyme, Mn^{2+}, and nucleotide is described by six equilibrium constants, which are defined in Table IV. The dissociation constant of the binary Mn^{2+} complexes (K_I) of 3′,5′-pdTp and 5′-TMP and those of the binary Mn^{2+}–enzyme complexes (K_D) were determined by EPR (Table III). To determine K_A', the dissociation constant of Mn^{2+} from ternary enzyme–Mn^{2+}–

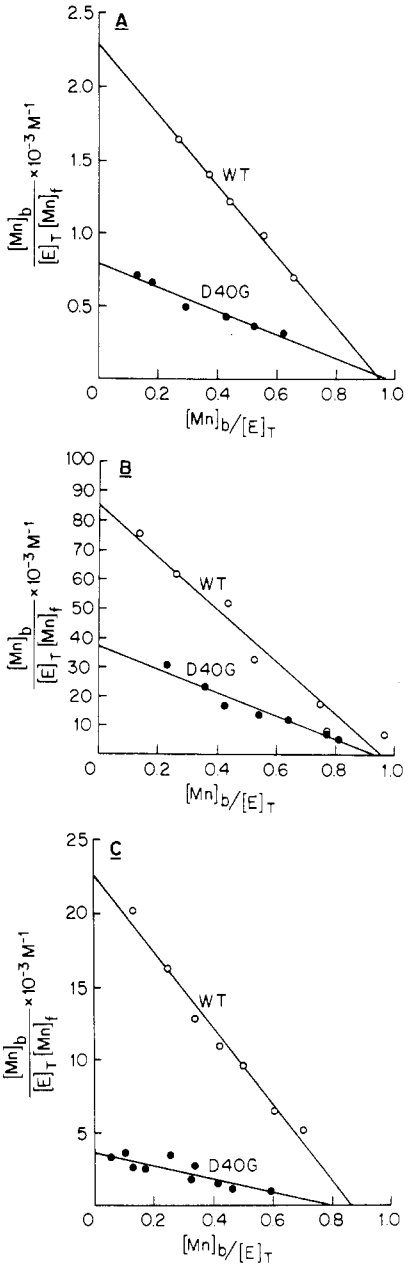

FIGURE 5: Scatchard plots of Mn^{2+} binding to the wild-type and D40G mutant of staphylococcal nuclease in the absence or in the presence of nucleotides. (A) Titration of wild-type enzyme and the D40G mutant of the staphylococcal nuclease with Mn^{2+}. The solution contained either 179 μM wild-type (○) or 235 μM D40G mutant (●) enzyme and 40 mM Tris-HCl, pH 7.4. (B) Titration of wild-type enzyme and the D40G mutant of staphylococcal nuclease with Mn^{2+} in the presence of 3′,5′-pdTp. Solutions contained 85 μM 3′,5′-pdTp, either 85 μM wild-type (○) or 84 μM D40G mutant enzyme (●), and 40 mM Tris-HCl, pH 7.4. (C) Titration of the wild-type enzyme and the D40G mutant of staphylococcal nuclease with Mn^{2+} in the presence of 5′-TMP. Solutions contained 102 μM 5′-TMP, either 107 μM wild-type (○) or 104 μM D40G mutant enzyme (●), and 40 mM Tris-HCl, pH 7.4. In (A)–(C), the free Mn^{2+} concentration was determined by EPR spectroscopy, and the lines represent linear least-squares fits to the data points. The symbols $[Mn]_b$, $[Mn]_f$, and $[E]_T$ represent bound Mn^{2+}, free Mn^{2+}, and the total enzyme concentrations, respectively.

nucleotide complexes, staphylococcal nuclease was titrated with Mn^{2+} in the presence of either 3′,5′-pdTp or 5′-TMP, measuring the free Mn^{2+} by EPR and the effects of the bound Mn^{2+} on $1/T_1$ of water protons.

From Scatchard plots of the EPR data (Figure 5B), K_A' of Mn^{2+} from the ternary pdTp complex of the mutant enzyme

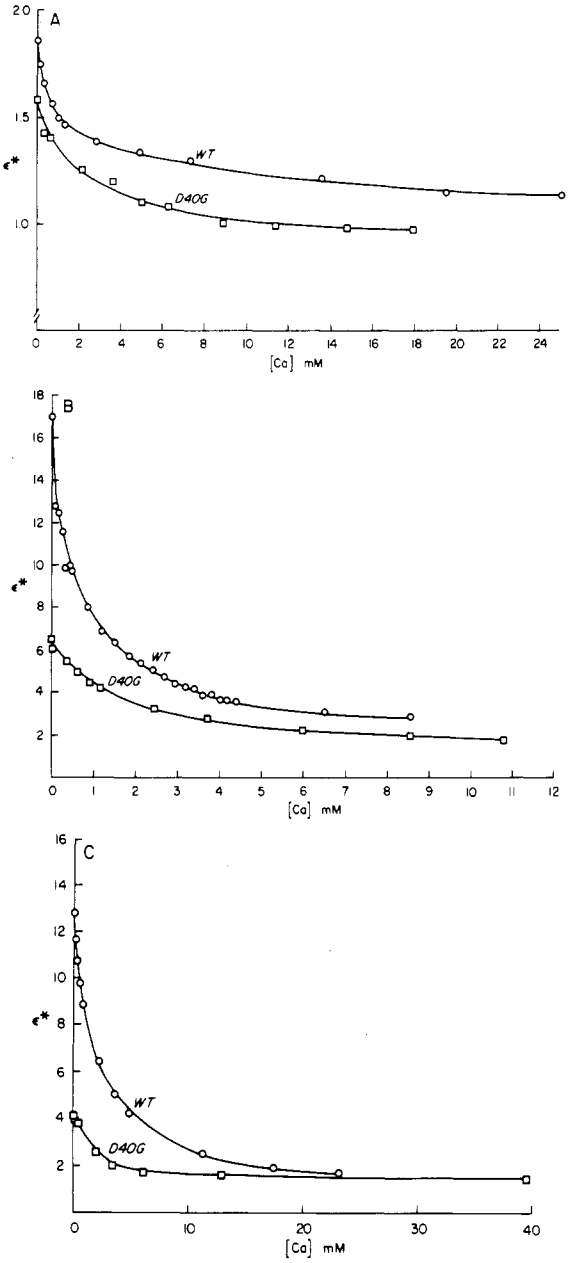

FIGURE 6: Displacement of Mn^{2+} by Ca^{2+} in complexes of the wild-type enzyme and the D40G mutant of staphylococcal nuclease detected by changes in the enhancement (ϵ^*) of the effects of Mn^{2+} on $1/T_1$ of water protons. (A) Displacement of Mn^{2+} by Ca^{2+} from the binary Mn^{2+} complex of the wild-type or the D40G mutant enzyme. Solutions contained either 179 μM wild-type enzyme with 332 μM Mn^{2+} (○) or 210 μM D40G mutant with 331 μM Mn^{2+} (□) as well as 40 mM Tris-HCl, pH 7.4. From the concentration of free Ca^{2+} at the midpoint of the titration, $[Ca^{2+}]_{1/2}$, K_D^{Ca} was calculated with the relationship $K_D^{Ca} = [Ca^{2+}]_{1/2}/(1 + [Mn^{2+}]/K_D^{Mn})$, where K_D^{Mn} is the dissociation constant of Mn^{2+} from the binary enzyme–Mn^{2+} complex (Table III). (B) Displacement of Mn^{2+} by Ca^{2+} from the ternary enzyme–Mn^{2+}–pdTp complexes of the wild-type or the D40G mutant staphylococcal nuclease. Solutions contained 85 μM 3′,5′-pdTp and either 85 μM wild-type enzyme with 60 μM Mn^{2+} (○) or 84 μM D40G mutant with 60 μM Mn^{2+} (□). (C) Displacement of Mn^{2+} by Ca^{2+} from ternary enzyme–Mn^{2+}–5′-TMP complexes of the wild-type enzyme and the D40G mutant of staphylococcal nuclease. The solutions contained 210 μM 5′-TMP and either 154 μM wild-type enzyme with 158 μM Mn^{2+} (○) or 218 μM D40G mutant enzyme with 169 μM Mn^{2+} (□). In (A)–(C), Ca^{2+} additions were done from concentrated stock solutions, which also contained all of the components of the titration solutions at the same final concentrations. Temperature was 23.5 °C. In (B) and (C) from the concentration of free Ca^{2+} at the midpoint of the titration, $[Ca^{2+}]_{1/2}$, $K_A'^{Ca}$ was calculated with the relationship $K_A'^{Ca} = [Ca^{2+}]_{1/2}/(1 + [Mn^{2+}]/K_A'^{Mn})$, where $K_A'^{Mn}$ represents the dissociation constant of Mn^{2+} from the ternary enzyme–metal–nucleotide complex (Table IV).

(25.1 ± 2.9 μM; Table IV) is only 2.3-fold greater than that of the wild-type enzyme (11.1 ± 0.6 μM; Table IV). Scatchard analysis of the $1/T_1$ data (not shown) yielded similar values of K_A' (Table IV). The K_A' values measured in the binding studies with enzyme and 3′,5′-pdTp (Table IV) are comparable to the K_I values of Mn^{2+} determined kinetically, at saturating levels of DNA (Table II). By comparing the K_D and K_A' values, it is concluded that 3′,5′-pdTp tightens the binding of Mn^{2+} to the mutant and wild-type enzymes by factors of 31 and 47, respectively (Tables III and IV). From Mn^{2+} titrations of the enzymes in the presence of 5′-TMP (Figure 5C), it is clear that Mn^{2+} binds more weakly in the ternary complexes of 5′-TMP than of pdTp, but a 5-fold greater K_A' value is noted for the mutant than for the wild-type enzyme (Table IV). 5-TMP raises the affinities of wild-type and mutant enzymes for Mn^{2+} by factors of 6.8 and 4.4, respectively (Tables III and IV).

(*B*) *Titrations with Nucleotides.* The most direct way of determining K_3, the dissociation constant of the nucleotide from the ternary enzyme–Mn^{2+}–nucleotide complex, is by titration of solutions of enzyme and Mn^{2+} with nucleotides, measuring changes in the enhancement of $1/T_{1p}$ of water protons (Mildvan & Engle, 1972). Such titrations, fit by computed curves (Figure 7), yielded the average K_3 values given in Table IV. Little effect of the mutation on the K_3 values of the nucleotides is seen (Table IV), in accord with the small difference in the K_M of DNA with the D40G and wild-type enzymes as detected kinetically (Table II).

The computer fitting of the nucleotide titrations (Figure 7) required values for K_S, the dissociation constants for the binary enzyme–nucleotide complexes. These are found by trial and error and can therefore be considered only as approximations. Nevertheless, independent measurements of the K_S of 3′,5′-pdTp by its competitive displacement of ϵpAp, monitoring the increase in fluorescence of the latter nucleotide, yielded K_S values in good agreement with those obtained by computer analysis and reveal little difference between the wild-type and mutant enzymes (Table IV). The K_S of pdTp, which we have measured for the wild-type enzyme (95 ± 30 μM), is in reasonable agreement with that found by equilibrium dialysis under somewhat different conditions (38 ± 10 μM; Dunn & Chaiken, 1975). Independent measurements of K_S could not be made with 5′-TMP since the high concentrations required of this weaker binding nucleotide obscured the fluorescence of ϵpAp by the inner filter effect. Hence, little significance is attached to the apparent difference in the K_S values of 5′-TMP for the wild-type and mutant enzymes.

Comparisons of K_3 and K_S (Table IV) reveal that Mn^{2+} raises the affinities of both wild-type and mutant enzymes for nucleotides, by 1 or 2 orders of magnitude at pH 7.4. Larger effects of Ca^{2+} on nucleotide binding to the wild-type enzyme have been detected at pH 8.8 (Cuatrecasas et al., 1967).

Table V compares the dissociation constants of various enzyme complexes measured in binding studies with those obtained by kinetic analysis. In general, the agreement is satisfactory. While the D40G mutation lowers the affinity of staphylococcal nuclease for metals, it does not greatly alter the affinity of the enzyme for its substrate DNA, or for nucleotide analogues.

The dissociation constant of the metal–nucleotide from the ternary complex (K_2) is derived from the relationship $K_2 = K_3K_D/K_1$ (Table IV). While little difference in the K_2 of the enzyme–Mn^{2+}–pdTp complex between mutant and wild-type enzymes is seen, a (4.3 ± 1.7)-fold greater K_2 of the enzyme–Mn^{2+}–TMP complex is seen with the D40G enzyme.

Table IV: Dissociation Constants (μM) and Enhancement Factors of $1/T_{1p}$ in Ternary Enzyme–Mn^{2+}–Nucleotide Complexes of Staphylococcal Nuclease[a]

		K_A'		K_S		K_3	K_2	
enzyme	nucleotide	EPR	$1/T_{1p}$[b]	fluorescence[c]	$1/T_{1p}$[d]	$1/T_{1p}$[d]	$1/T_{1p}$[d]	ϵ_T[d]
wild type	3′,5′-pdTp	11.1 ± 0.6	17 ± 2	95 ± 22	94 ± 38	2.5 ± 1.0	2.2 ± 0.9	24.8 ± 0.4
	5′-TMP	38.0 ± 3.6	64 ± 8		191 ± 66	17.4 ± 6.3	1.76 ± 0.60	18.0 ± 0.8
mutant (D40G)	3′,5′-pdTp	25.1 ± 2.9	22.6 ± 2.6	60 ± 35	61 ± 30	1.2 ± 0.6	3.2 ± 1.7	8.1 ± 0.6
	5′-TMP	218 ± 34	259 ± 22		827 ± 169	25.1 ± 5.8	7.6 ± 1.7	13.1 ± 1.5

[a] The dissociation constants of the ternary and relevant binary complexes of enzyme (E), metal (M), and ligands (L), are defined as follows: K_1 = [M][L]/[M–L]; K_D = [E][M]/[E–M]; K_2 = [E][M–L]/[E–M–L]; K_A' = [E–L][M]/[E–M–L]; K_3 = [E–M][L]/[E–M–L]; K_S = [E][L]/[E–L]. Note that $K_1K_2 = K_3K_D = K_A'K_S$. [b] Determined by $1/T_{1p}^*$ of water protons in Mn^{2+} titrations. [c] Measured from titrations monitoring the increase in fluorescence of 3′,5′-ϵpAp when it was displaced by 3′,5′-pdTp, using the measured K_S values of 3′,5′-ϵpAp of 70 ± 36 and 60 ± 40 μM for the wild-type and mutant enzymes, respectively. [d] Determined by computer analysis of nucleotide titrations (Reed et al., 1970; Mildvan & Engle, 1972).

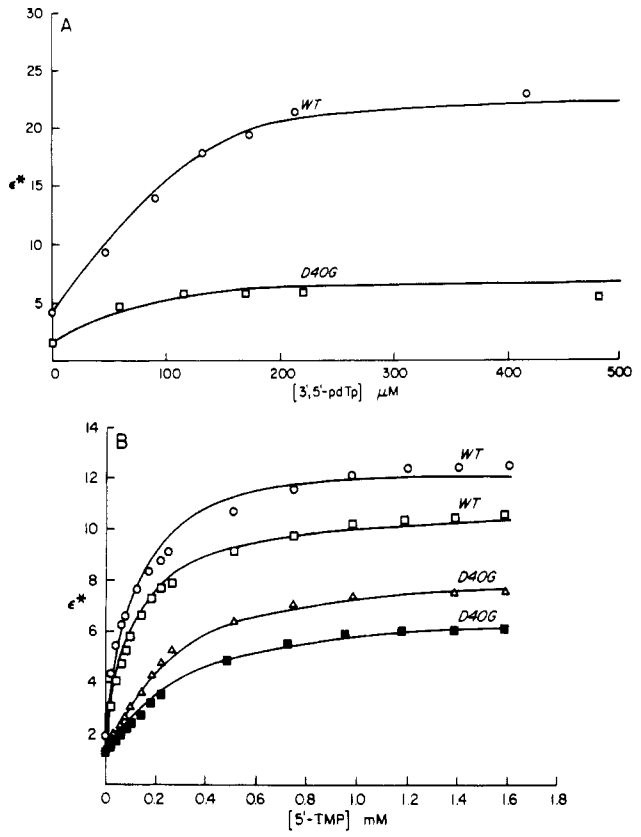

FIGURE 7: Nucleotide binding studies to Mn^{2+} complexes of wild-type enzyme and the D40G mutant of staphylococcal nuclease, measuring the changes in the enhancement (ϵ^*) of the paramagnetic effects of Mn^{2+} on $1/T_1$ of water protons. (A) Titrations of Mn^{2+} complexes of the wild-type and D40G mutant enzymes with 3′,5′-pdTp. Solutions contained either 488 μM wild-type enzyme with 106 μM Mn^{2+} (○) or 391 μM D40G mutant enzyme with 100 μM Mn^{2+} (□). (B) Titrations of Mn^{2+} complexes of the wild-type and D40G mutant enzymes with 5′-TMP. Solutions contained 95 μM wild-type enzyme with 24 μM Mn^{2+} (○), 95 μM wild-type enzyme with 61 μM Mn^{2+} (□), 83 μM D40G mutant enzyme with 24 μM Mn^{2+} (△), and 83 μM D40G mutant enzyme with 49 μM Mn^{2+} (■). In (A) and (B), nucleotides were added from concentrated stock solutions, which also contained the other components of the titration at the same final concentrations. Other components and conditions were as described in Figure 6. In both (A) and (B), the data points are shown together with curves computed, using the parameters given in Tables III and IV.

Significant decreases in ϵ_T, the enhancement of the ternary complexes, are found with the mutant enzyme in both the pdTp and the 5′-TMP complexes (Table IV), indicating structural differences in the Mn^{2+} coordination sphere on the mutant enzyme.

Ternary Ca^{2+} Complexes of Wild-Type and D40G Enzymes with Nucleotide Substrate Analogues. Titrations of ternary enzyme–Mn^{2+}–nucleotide complexes with Ca^{2+} were carried out by measuring the decrease in $1/T_{1p}$ of water protons (Figure 6). This decrease resulted from the displacement of Mn^{2+} by Ca^{2+} as independently established by EPR, which showed the appearance of free Mn^{2+}. Analysis of these titrations yielded dissociation constants (K_A') of Ca^{2+} from the ternary E–Ca^{2+}–5′-TMP and E–Ca^{2+}–3′,5′-pdTp complexes of both the wild-type and D40G enzymes. The K_A' values were 3–4-fold weaker in the mutant enzyme (Table VI). These K_A' values, together with those of K_D (Table III) and K_S (Table IV), yielded K_3 values for the ternary Ca^{2+} complexes that were (3 ± 1)-fold weaker for the 5′-TMP complex of the mutant. The mutations did not significantly alter the K_3 of 3′,5′-pdTp (Table VI).

Completion of the analysis of the thermodynamics of the ternary complexes of Ca^{2+} required values of the dissociation constants (K_1) of the binary Ca^{2+}–nucleotide complexes. These were determined by EPR measurements in competition with Mn^{2+} (Table III). The values of K_1 together with those of K_A' and K_S yielded equilibrium constants (K_2) for the dissociation of Ca^{2+}–5′-TMP and Ca^{2+}–3′,5′-pdTp from their respective ternary complexes (Table VI). The K_2 values, which measures the combined effects of the mutation on both metal binding and nucleotide binding, is 12-fold greater in the mutant for Ca^{2+}–5′-TMP and 2.3-fold greater in the mutant for Ca^{2+}–3′,5′-pdTp, although the latter difference may not be significant due to the propagation of errors in the calculation of K_2 (Table VI). It is of interest that even smaller effects of the D40G mutation on K_2 are noted with the inhibitory metal, Mn^{2+} (Table IV).

Frequency Dependence of $1/T_{1p}$ of Water Protons with Binary and Ternary Mn^{2+} Complexes of Staphylococcal Nuclease. The 31-fold decrease in V_{max} of the D40G mutant of staphylococcal nuclease as compared to the wild-type enzyme (Table II) indicates a significant structural differences in the metal complex of the mutant enzyme. Evidence for such a structural difference in the coordination sphere of the metal in the binary and ternary Mn^{2+} complexes is manifested by significantly lower enhancement values with the mutant enzyme, as compared to the wild-type enzyme (Tables III and IV). An analysis of the frequency dependence of $1/T_{1p}$ of water protons was carried out to determine the basis for the lower relaxivity of Mn^{2+} when bound to the mutant enzyme (Table VII). The most consistent difference between the Mn^{2+} complexes of wild-type and mutant enzymes is a shorter correlation time in the mutant, resulting primarily from an increase in B, the zero-field splitting parameter, indicating a decreased symmetry in the ligand field at Mn^{2+} when bound to the mutant enzyme. This is consistent with the X-ray structure, which shows a pseudo 3-fold axis of symmetry about the metal in the wild-type enzyme due to three cis ligands donated by the protein (Figure 1) (Cotton et al., 1979). This symmetry would be lost in the D40G mutant, in which the

Table V: Comparison of Dissociation Constants (μM) and Kinetic Parameters of Ca^{2+} and Mn^{2+} in Binary and Ternary Complexes of Staphylococcal Nuclease

enzyme	K_A^{Ca} (kinetics)	K_D^{Ca} (binding)	K_M^{Ca} (kinetics)	$K_A'^{Ca}$ (binding)	K_I^{Mn} (kinetics)	$K_A'^{Mn}$ (binding)	K_S^{DNA} (kinetics)[e]	$K_S^{5'\text{-TMP}}$ (binding)	K_S^{pdTp} (binding)	K_M^{DNA} (kinetics)[e]	$K_3^{5'\text{-TMP}}$[f] (binding)	K_3^{pdTp}[f] (binding)
wild type	460 ± 60	510 ± 70	110 ± 20	71 ± 8[a]	6.8 ± 4.2	11.1 ± 0.6[a]	12.8 ± 0.5	191 ± 66[c]	94 ± 38[c]	2.5 ± 0.6	121 ± 47	13.1 ± 5.8
				324 ± 35[b]		38.0 ± 3.6[b]			95 ± 21.5[d]			
mutant (D40G)	3440 ± 360	1660 ± 300	1330 ± 70	259 ± 33[a]	105 ± 15	25.1 ± 2.9[a]	19.9 ± 2.4	827 ± 169[c]	61 ± 30[c]	3.3 ± 0.9	453 ± 144	9.5 ± 5.1
				910 ± 149[b]		218 ± 34[b]			60 ± 35[d]			

[a] Determined by using 3′,5′-pdTp. [b] Determined by using 5′-TMP. [c] Determined by PRR and computer analysis (Reed et al., 1970; Mildvan & Engle, 1972). [d] Determined by fluorescence measurements. [e] Expressed as micromolar, assuming the molecular weight of the substrate to be an average tetranucleotide of M_r 1400. Hence, the values are probably upper limits. [f] Calculated for enzyme–Ca^{2+}–nucleotide complexes from Mn^{2+} displacement experiments.

Table VI: Dissociation Constants (μM)[a] of Ternary Enzyme–Ca^{2+}–Nucleotide Complexes of Staphylococcal Nuclease

enzyme	nucleotide	K_A'	K_3	K_2
wild type	3′,5′-pdTp	71 ± 8	13.1 ± 5.8	5.6 ± 1.9
	5′-TMP	324 ± 35	121 ± 47	12.1 ± 7.4
mutant (D40G)	3′,5′-pdTp	259 ± 33	9.5 ± 5.1	13 ± 7
	5′-TMP	910 ± 149	433 ± 144	148 ± 82

[a] The dissociation constants of the ternary and relevant binary complexes of enzyme, metal, and ligands are defined in Table IV. The K_1 values are given in Table III, and the K_S values are given in Table IV.

Asp-40 ligand is presumably replaced by a water ligand. Another difference between the Mn^{2+} complexes of the wild-type and mutant enzymes is a decrease in τ_μ, a time constant for motion of the water ligands of the metal (Bloembergen & Morgan, 1961; Friedman, 1977), suggesting less steric hindrance and greater mobility of the coordination sphere in the mutant. Estimates of q, the coordination number for fast-exchanging water ligands on bound Mn^{2+} in the various enzyme–Mn^{2+} complexes (Table VII), are significantly lower than predicted from the X-ray structure (Figure 1) except in the case of the ternary pdTp complex of the wild-type enzyme. These findings suggest that one to three water ligands on enzyme-bound Mn^{2+}, including the additional water ligand on Mn^{2+} in the complexes of D40G, exchange slowly with the bulk solvent.

Discussion

The observed thermodynamic effects of mutating Asp-40 of staphylococcal nuclease to Gly are in accord with the X-ray structure of this enzyme (Cotton et al., 1979). Thus the loss of one of the three cis ligands donated by the protein to the essential metal activator Ca^{2+} results in a (5 ± 2)-fold lower affinity of the enzyme for Ca^{2+} as detected either kinetically as the activator constant K_A^{Ca} (Table II) or nonkinetically in binding studies as K_D^{Ca} (Table III). Similarly, the mutant enzyme binds the competitive inhibitor Mn^{2+} 3 times weaker than does the wild-type enzyme as detected by two independent binding studies (Table III). The binding of the substrate DNA amplifies these differences in metal affinity between the enzymes since K_M^{Ca} is 10-fold greater and K_I^{Mn} is 15-fold greater in the mutant as compared to the wild-type enzyme (Table II). This amplification results from the fact that DNA tightens the binding of metals to the wild-type enzyme by somewhat larger factors than to the mutant enzyme. The simple nucleotide competitive inhibitors 3′,5′-pdTp and 5′-TMP do not amplify the difference in metal affinities between the mutant and wild-type enzymes, as may be seen by comparing the corresponding K_A' values (Tables III and IV), although they do significantly raise the affinities of both enzymes for Ca^{2+} and Mn^{2+}. This is because for a given metal and nucleotide equal effects are exerted on the affinities of the mutant and wild-type enzymes for metals. The D40G mutation has little effect on the affinity of staphylococcal nuclease for the DNA substrate or for nucleotide substrate analogues as may be seen by comparing the K_S values of the various binary complexes (Tables II and IV) and the K_3 values of the ternary complexes (Tables II, IV, and VI). These results are also consistent with the X-ray structure, which shows Asp-40 to interact with the metal but not with 3′,5′-pdTp (Figure 1). As summarized in Table V, dissociation constants of Ca^{2+} and Mn^{2+} from their respective binary and ternary complexes, obtained by kinetic analyses, show reasonable agreement with those measured in direct binding studies. The DNA substrate binds to staphylococcal nuclease and to its metal complexes more tightly than do simple nucleotides at pH 7.4 (Table V), probably due to a greater number of interactions with the protein, as has

Table VII: Analysis of Frequency Dependence of Longitudinal Relaxation Rates of Water Protons in the Presence of Mn^{2+} Complexes of Staphylococcal Nuclease[a]

	frequency (MHz)									
	80	100	250	250	80	100	250			
complex	$1/(fT_{1p})$ ($\times 10^{-6}$ s^{-1})	$1/(fT_{1p})$ ($\times 10^{-6}$ s^{-1})	$1/(fT_{1p})$ ($\times 10^{-6}$ s^{-1})	$1/(fT_{2p})$ ($\times 10^{-6}$ s^{-1})[b]	τ_c ($\times 10^9$ s)	τ_c ($\times 10^9$ s)	τ_c ($\times 10^9$ s)	B ($\times 10^{-21}$ s^{-2})	τ_v ($\times 10^{13}$ s)	q
wild type–Mn^{2+}	0.728	0.687	0.347	22.1	0.693	0.707	0.900	0.95	3.15	0.8 ± 0.1
wild type–Mn^{2+}–3′,5′-pdTp	2.84	2.03	0.737	18.6	1.07	1.07	1.16	1.13	1.67	2.2 ± 0.5
wild type–Mn^{2+}–5′-TMP	1.63	1.27	0.472	14.3	1.00	1.00	1.05	1.70	1.19	1.3 ± 0.3
D40G–Mn^{2+}	0.514	0.477	0.265	8.52	0.659	0.659	0.777	1.26	2.51	0.6 ± 0.1
D40G–Mn^{2+}–3′,5′-pdTp	2.03	1.61	0.519	13.5	1.26	1.26	1.31	1.51	1.06	1.5 ± 0.2
D40G–Mn^{2+}–5′-TMP	0.949	0.624	0.304	9.19	0.792	0.793	0.817	2.54	1.00	0.9 ± 0.2

[a] The normalized longitudinal relaxation rates of water protons $[1/(fT_{1p})]$ as a function of the precession frequencies of protons (ω_I) and unpaired electrons (ω_S) were analyzed according to the following equations (Mildvan & Gupta, 1978): $1/(fT_{1p}) = q(C/r)^6([3\tau_c(1 + \omega_I^2\tau_c^2) + 7\tau_c/(1 + \omega_S^2\tau_c^2)]$ and $1/\tau_c \sim 1/\tau_S = B[\tau_v/(1 + \omega_S^2\tau_v^2) + 4\tau_v/(1 + \omega_S^2\tau_v^2)]$, where q is the number of fast exchanging water ligands, C is a product of physical constants equal to 812 Å/$s^{1/3}$ for Mn^{2+}–proton interactions, τ_c is the dipolar correlation time, τ_S is the longitudinal electron spin relaxation time, B is the zero-field splitting parameter, and τ_v is a time constant for motion of the water ligands that modulates B. [b] $1/(fT_{2p})$ is the normalized transverse relaxation rate of water protons.

previously been shown by kinetic studies at pH 8.8 (Cuatrecasas et al., 1968).

Our kinetic and binding studies reveal that Mn^{2+} competes linearly with the activating Ca^{2+} ion, shows lower affinity for the D40G mutant as does Ca^{2+}, and exerts qualitatively similar effects as Ca^{2+} on nucleotide binding, indicating that Mn^{2+} occupies the Ca^{2+} site. Despite these similarities, Mn^{2+} is at least 6000 times less effective in activating the enzyme and may well not activate at all. Possible reasons are the smaller radius of Mn^{2+} (Cotton & Wilkinson, 1980), its greater electrophilicity (Sillen & Martell, 1964), and slower ligand exchange rates (Eigen & Wilkins, 1965), rendering it more difficult for the phosphodiester substrate to enter the inner coordination sphere of the Mn^{2+}. Second-sphere Mn^{2+}–nucleotide complexes on the enzyme are suggested by the unaltered q values in the ternary enzyme–Mn^{2+}–nucleotide complexes (Table VII) and by preliminary distance measurements with ^{31}P NMR.[2] Alternatively, Mn^{2+}, upon binding, may distort the enzyme to an inactive conformation.

An unexpected finding in these studies was the 31-fold lower maximal velocity of the D40G mutant enzyme, at saturating levels of both Ca^{2+} and DNA. The addition of formate to the D40G assay medium did not restore activity, suggesting an explanation other than the simple loss of a negative charge near the Ca^{2+}. Removal of one of the three cis ligands donated to Ca^{2+} by the protein has very likely altered the structure of the active ternary enzyme–Ca^{2+}–DNA complex. A clue to the nature of this structural alteration is provided by the frequency dependences of the effects of the Mn^{2+}–enzymes on $1/T_{1p}$ of water protons (Table VII), which reveal a decrease in τ_c, the correlation time for the Mn^{2+}–H_2O dipolar interaction. This decrease in τ_c results from a decrease in both the symmetry (B) and rigidity (τ_v) of the ligands of Mn^{2+}. The decrease in the symmetry of the ligands around the metal in the complexes of the mutant enzyme presumably results from the loss of the pseudo 3-fold symmetry axis (Figure 1). Such a loss of symmetry in the enzyme–Ca^{2+}–DNA complex could decrease the activity in several ways. Alteration in the position of Ca^{2+}, increasing its distance from the phosphodiester group of the substrate, could weaken this important interaction. An increase in the distance of Ca^{2+} from Glu-43, which may act as a general base (Cotton et al., 1979),[3] could weaken the binding of the attacking water molecule. The alignment of reactants or the overall geometry of the active site could also be perturbed by a change in the position of the Ca^{2+}. A decrease in the rigidity at the active site resulting from the loss of an enzymatic ligand to Ca^{2+} could slow the catalytic rate by raising the entropy barrier to the reaction (Mildvan, 1974). Further studies are in progress to examine these possibilities in greater detail.

[2] E. H. Serpersu, D. Shortle, and A. S. Mildvan, unpublished observations.

[3] J. A. Gerlt, personal communication.

ACKNOWLEDGMENTS

We are grateful to Tian Y. Tsong and Ludwig Brand for permitting us to use their spectrofluorometers and to Terry Fox for skilled technical assistance.

Registry No. 3′,5′-pdTp, 2863-04-9; 5′-TMP, 365-07-1; Ca, 7440-70-2; Mn, 7439-96-5; staphylococcal nuclease, 9013-53-0.

REFERENCES

Bloembergen, N., & Morgan, L. O. (1961) *J. Chem. Phys. 34*, 842.

Carr, H. Y., & Purcell, E. M. (1954) *Phys. Rev. 94*, 630.

Cohn, M., & Townsend, J. (1954) *Nature (London) 173*, 1090.

Cotton, F. A., & Wilkinson, G. (1980) *Advanced Inorganic Chemistry*, p 14, Wiley, New York.

Cotton, F. A. Hazen, E. E., Jr., & Legg, M. J. (1979) *Proc. Natl. Acad. Sci. U.S.A. 76*, 2551.

Cuatrecasas, P., Fuchs, S., & Anfinsen, C. B. (1967) *J. Biol. Chem. 242*, 1541.

Cuatrecasas, P., Wilchek, M., & Anfinsen, C. B. (1968) *Science (Washington, D.C.) 162*, 1491.

Dunn, B. M., DiBello, C., & Anfinsen, C. B. (1973) *J. Biol. Chem. 248*, 4769.

Eigen, M., & Wilkins, R. G. (1965) *Adv. Chem. Ser. No. 49*, 55.

Friedman, H. L. (1977) in *Protons and Ions Involved in Fast Dynamic Phenomena* (Laszlo, P., Ed.) p 27, Elsevier, New York.

Mildvan, A. S. (1974) *Annu. Rev. Biochem. 43*, 357.

Mildvan, A. S., & Cohn, M. (1963) *Biochemistry 2*, 910.

Mildvan, A. S., & Cohn, M. (1966) *J. Biol. Chem. 241*, 1178.

Mildvan, A. S., & Engle, J. L. (1972) *Methods Enzymol. 26C*, 654.

Mildvan, A. S., & Gupta, R. K. (1978) *Methods Enzymol. 49G*, 322.

Reed, G. H., Cohn, M., & O'Sullivan, W. J. (1970) *J. Biol. Chem. 245*, 6547.

Reuben, J., & Cohn, M. (1970) *J. Biol. Chem. 245*, 6539.

Serpersu, E. H., Shortle, D. R., & Mildvan, A. S. (1985) *Abstracts of Papers*, 190th National Meeting of the Am-

erican Chemical Society, Chicago, Sept 8–13, 1985, American Chemical Society, Washington, D.C.
Shortle, D. (1983) *Gene 22*, 181.
Shortle, D., & Lin, B. (1985) *Genetics 110*, 539.
Sillen, L. G., & Martell, A. E. (1964) *Spec. Publ.–Chem. Soc. 17*.
Slater, J. P., Tamir, I., Loeb, L. A., & Mildvan, A. S. (1972) *J. Biol. Chem. 247*, 6784.
Tucker, P. W., Hazen, E. E., Jr., & Cotton, F. A. (1978) *Mol. Cell. Biochem. 22*, 67.
Tucker, P. W., Hazen, E. E., Jr., & Cotton, F. A. (1979) *Mol. Cell. Biochem. 23*, 3.

^{31}P NMR Saturation Transfer Measurements of Phosphorus Exchange Reactions in Rat Heart and Kidney in Situ†

Alan P. Koretsky,‡,§ Samuel Wang,‖ Melvin P. Klein,§ Thomas L. James,⊥,# and Michael W. Weiner*,‡,‖,#
Medical Service, Veterans Administration Medical Center, San Francisco, California 94121, Chemical Biodynamics Division, Lawrence Berkeley Laboratory, University of California, Berkeley, California 94720, and Departments of Medicine, Pharmaceutical Chemistry, and Radiology, University of California, San Francisco, California 94133
Received February 19, 1985; Revised Manuscript Received July 29, 1985

ABSTRACT: ^{31}P NMR spectra of rat kidney and heart, in situ, were obtained at 97.2 MHz by using chronically implanted radio-frequency coils. Previous investigators have used magnetization transfer techniques to study phosphorus exchange in perfused kidney and heart. In the current experiments, saturation transfer techniques were used to measure the steady-state rate of exchange between inorganic phosphate (P_i) and the γ-phosphate of ATP (γATP) in kidney, and between phosphocreatine (PCr) and γATP, catalyzed by creatine kinase, in heart. The rate constant for the exchange detected between P_i and γATP in kidney, presumably catalyzed by oxidative phosphorylation, was 0.12 ± 0.03 s^{-1}. This corresponds to an ATP synthesis rate of 12 μmol min^{-1} (g wet weight)$^{-1}$. Comparison of previously published O_2 consumption and Na^+ reabsorption rates for the intact kidney with the NMR-derived rate for ATP synthesis gave flux ratios of $J_{ATP}/J_{O_2} = 1.6$–3.3 and $J_{Na^+}/J_{ATP} = 4$–10. The rate constants for the creatine kinase reaction, assuming a simple two-site exchange, were found to be 0.57 ± 0.12 s^{-1} for the forward direction (PCr → ATP) and 0.50 ± 0.16 s^{-1} for the reverse direction (ATP → PCr). The forward rate (0.78 ± 0.18 intensity unit/s) was significantly larger ($p < 0.05$) than the reverse rate (0.50 ± 0.16 intensity unit/s). This difference between the forward and reverse rates of creatine kinase has been previously noted in the perfused heart. The difference has been attributed to participation of ATP in other reactions. To test this possibility, the reverse rate was measured by saturating both PCr and the β-phosphate of ATP. The rate obtained in this manner was not significantly different from that derived by assuming a two-site exchange. These results suggest the possibility that compartmentation of ATP might be responsible for the difference in rates.

A detailed understanding of the regulation and control of metabolic pathways requires an estimiate of the rates of each individual reaction. For the case of the generation of ATP by oxidative phosphorylation and utilization for various work functions (e.g., Na^+ transport and muscle contraction), most kinetic information comes from in vitro studies of isolated subcellular systems (Hansford, 1980). However, functioning of regulatory mechanisms in vivo may be altered in vitro. Physiologic experiments performed on intact tissue have produced information concerning the coupling of oxidative metabolism to work demands (Mandel & Balaban, 1981). These studies have had to rely on assumptions concerning detailed reaction mechanisms, such as the stoichiometry of ATP formation from oxidative phosphorylation. To bridge the gap between in vitro studies of isolated mitochondria and physiologic studies, it is important to know the rate of metabolic reactions, such as ATP formation and utilization, in vivo.

NMR techniques can be used to measure the rates of enzyme reactions in vivo (Brown et al., 1977; Gupta, 1979). In particular, by use of ^{31}P NMR magnetization transfer techniques, the rate of the creatine kinase reaction has been measured in perfused heart (Brown et al., 1977; Matthews et al., 1982; Nunally & Hollis, 1979), isolated muscle (Brown et al., 1979; Gadian et al., 1981), and rat and turtle brain in situ (Balaban et al., 1983; Shoubridge et al., 1982; Wemmer et al., 1982). Additionally, the rate of ATP synthesis has been measured in the perfused heart and kidney (Freeman et al., 1983; Matthews et al., 1981; Yahaya et al., 1984) as well as the rat brain (Shoubridge et al., 1982) and maize root tips (Roberts et al., 1984).

Techniques have been developed in this laboratory which allow ^{31}P NMR spectra to be obtained from rat kidney, heart, and liver in situ (Weiner et al., 1980; Koretsky et al., 1982, 1983). The stability of the animals and the high metabolic rates which occur in these organs in situ offer advantages over

† This work was supported by National Institutes of Health Grant AM 3392-01A1, the Veterans Administration Medical Research Services, the Research and Education Allocation Committee and Faculty Senate Research Committee of U.C.S.F., the Hedco Foundation, the Northern California Heart Association, and the Office of Energy Research, Office of Health and Environmental Research, Health Effects Research Division of the U.S. Department of Energy, under Contract DE-AC03-765-F00098.
* Address correspondence to this author at the Veterans Administration Medical Center, University of California, San Francisco.
‡ Veterans Administration Medical Center.
§ University of California, Berkeley.
‖ Department of Medicine, University of California, San Francisco.
⊥ Department of Pharmaceutical Chemistry, University of California, San Francisco.
Department of Radiology, University of California, San Francisco.

0006-2960/86/0425-0077$01.50/0